Available online at www.sciencedirect.com
ScienceDirect
Radiation Physics and Chemistry 77 (2008) 207–214
Radiation Physics and Chemistry
www.elsevier.com/locate/radphyschem

# Bremsstrahlung cross-section with screening and Coulomb corrections at high energies

Eberhard Haug*

*Institut für Astronomie und Astrophysik, Universität Tübingen, Auf der Morgenstelle 10, D-72076 Tübingen, Germany*

Received 8 June 2007; accepted 9 October 2007

**Abstract**

Using analytical formulae which are exact in Born approximation, the doubly differential bremsstrahlung cross-section with form-factor screening is calculated. For the atomic form factor parameters are applied which approximate self-consistent Dirac–Hartree–Fock–Slater calculations. The evaluation of the bremsstrahlung spectrum requires a single numerical integration. The results are superior to the customary Bethe approximation, in particular at the high-energy part of the spectrum. At high energies the screening correction can be added to any Coulomb-corrected cross-section without screening. In the present work, we are using a cross-section calculated by means of Sommerfeld–Maue functions with additional higher-order terms.


*PACS:* 12.20.Ds; 34.80.−i

*Keywords:* QED; Atomic collision processes; Bremsstrahlung

## 1. Introduction

The calculation of bremsstrahlung cross-sections is a problem of long standing. The most simple approach, the Born approximation for a pure Coulomb field (Bethe and Heitler, 1934; Heitler, 1954), yields poor results for targets with higher atomic numbers and near the short-wavelength limit of the spectrum. Therefore a number of calculations beyond the Born approximation have been performed. The main improvements refer to the Coulomb and screening corrections to the bremsstrahlung cross-section, in particular at high energies (Olsen, 1955; Olsen et al., 1957; Sørenssen, 1965; Seltzer and Berger, 1985; Al-Beteri and Raeside, 1989). Radiative corrections are usually small and are not considered here. The best available approach utilizes the relativistic partial-wave approximation to describe the motion of the electron in the static field of the target atom, and the multipole series expansion for the photon (Tseng and Pratt, 1971). However, the evaluation of the matrix element becomes computationally very intensive which imposes severe limitations on the energy range that can be handled.

In bremsstrahlung production the atomic screening of the nuclear Coulomb potential is very important for energetic incident electrons, especially in the low-energy part of the spectrum. As was shown by Olsen et al. (1957) the screening and Coulomb corrections of the bremsstrahlung cross-section integrated over the angles of the final electrons are additive and nearly independent of each other at high energies. Utilizing this property, the screening correction is calculated by means of the analytical formulae of Fronsdal and Überall (1958) which are exact in Born approximation. The Coulomb correction is taken into account by use of the cross section of Roche et al. (RDP, 1972) which was calculated with Sommerfeld–Maue (SM) wave functions supplemented by higher-order terms. This method is equivalent to the approach of Davies et al. (1954) and Olsen (1955), but without resorting to the high-energy and small-angle limits. Thus it is to be expected that the validity of the present formulae extends to lower energies.

In the following, relativistic units $\hbar = m = c = 1$ will be used, i.e., the energies of electrons and photons are

*Tel.: +49 7071 2975 942; fax: +49 7071 295889.
*E-mail address:* haug@tat.physik.uni-tuebingen.de

0969-806X/$ - see front matter © 2007 Elsevier Ltd. All rights reserved.
doi:10.1016/j.radphyschem.2007.10.003

expressed in units of the electron rest energy $mc^2$, and the momenta in units of $mc$, unless specified otherwise. Then the energy–momentum relation of electrons reads $\varepsilon^2 = p^2 + 1$ where $\varepsilon$ is the total energy including the rest energy. The unit of length is the Compton wavelength $\hbar/mc$. The energies of the incident and final electrons are designated by $\varepsilon_1$ and $\varepsilon_2$, respectively, the corresponding momenta by $\mathbf{p}_1$ and $\mathbf{p}_2$, and the photon momentum by $\mathbf{k}$. The recoil momentum of the target atom is $\mathbf{q} = \mathbf{p}_1 - \mathbf{p}_2 - \mathbf{k}$.

## 2. Atomic screening according to Fronsdal and Überall

Assuming spherical symmetry, the screening function $\Phi(r)$ is defined as the ratio between the electrostatic potential $U(r)$ experienced by an electron at a distance $r$ from the nucleus and the electrostatic potential of the bare nucleus (Salvat et al., 1987):

$$U(r) = -\frac{\alpha Z}{r}\,\Phi(r), \tag{1}$$

where $\alpha$ is the fine-structure constant and $Z$ the atomic number of the target atom. Screening functions are usually based on the Thomas–Fermi statistical model of the atom and its refinements. A few of them are founded on self-consistent Hartree–Fock or Hartree–Fock–Slater calculations (see Salvat et al., 1987, for references). Analytical approximations for the potential $U(r)$ often employ the superposition of Yukawa potentials in the form

$$U(r) = -\frac{\alpha Z}{r}\sum_i a_i\,\mathrm{e}^{-b_i r} \tag{2}$$

with $\sum a_i = 1$. The atomic electron density $\rho(r)$, normalized to $\alpha Z$, is connected to the screening function by Poisson's equation:

$$\Delta U(r) = -4\pi\rho(r) \tag{3}$$

resulting in

$$\rho(r) = \frac{\alpha Z}{4\pi r}\frac{\mathrm{d}^2\Phi}{\mathrm{d}r^2}. \tag{4}$$

The atomic screening of the nuclear Coulomb potential can be taken into account by multiplying the triply differential cross-section by $[1 - F(q,Z)]^2$ (Haug and Nakel, 2004), where the form factor is defined as

$$\begin{aligned} F(q,Z) &= \frac{1}{\alpha Z}\int \rho(r)\,\exp(\mathrm{i}\mathbf{q}\cdot\mathbf{r})\,\mathrm{d}^3 r \\ &= \sum_i \frac{a_i b_i^2}{q^2 + b_i^2} = 1 - \sum_i \frac{a_i q^2}{q^2 + b_i^2}. \end{aligned} \tag{5}$$

Moliére (1947) has approximated the Thomas–Fermi potential by Eq. (2)with

$$b_i = \frac{\beta_i}{121}Z^{1/3},\quad i = 1,2,3, \tag{6}$$

and

$$a_1 = 0.1,\quad a_2 = 0.55,\quad a_3 = 0.35,$$
$$\beta_1 = 6,\quad \beta_2 = 1.2,\quad \beta_3 = 0.3.$$

In the following calculations the screening parameters of Salvat et al. (1987) are used. These authors have derived analytical Dirac–Hartree–Fock–Slater screening functions for atoms with atomic numbers $Z = 1-92$ by fitting them to the same functional form as Moliére (1947), Eq. (2).[1] If the screening is described by the form factor (5), the bremsstrahlung cross-section differential in energy and solid angle of the photon is given by

$$\begin{aligned} \frac{\mathrm{d}^2\sigma}{\mathrm{d}k\,\mathrm{d}\Omega_k} &= \int \frac{\mathrm{d}^3\sigma}{\mathrm{d}k\,\mathrm{d}\Omega_k\,\mathrm{d}\Omega_{p_2}}\,[1 - F(q,Z)]^2\,\mathrm{d}\Omega_{p_2} \\ &= \int \frac{\mathrm{d}^3\sigma}{\mathrm{d}k\,\mathrm{d}\Omega_k\,\mathrm{d}\Omega_{p_2}}\left[\sum_{i=1}^{3}\frac{a_i q^2}{q^2 + b_i^2}\right]^2 \mathrm{d}\Omega_{p_2} \\ &= \int \frac{\mathrm{d}^3\sigma}{\mathrm{d}k\,\mathrm{d}\Omega_k\,\mathrm{d}\Omega_{p_2}}\,q^4\left\{\sum_{i=1}^{3}\frac{a_i^2}{(q^2 + b_i^2)^2}\right. \\ &\quad + \frac{2a_1a_2}{(q^2 + b_1^2)(q^2 + b_2^2)} \\ &\quad + \frac{2a_1a_3}{(q^2 + b_1^2)(q^2 + b_3^2)} \\ &\quad \left. + \frac{2a_2a_3}{(q^2 + b_2^2)(q^2 + b_3^2)}\right\} \\ &= \int \frac{\mathrm{d}^3\sigma}{\mathrm{d}k\,\mathrm{d}\Omega_k\,\mathrm{d}\Omega_{p_2}}\,q^4\left\{\sum_{i=1}^{3}\frac{a_i^2}{(q^2 + b_i^2)^2}\right. \\ &\quad + \frac{2a_1a_2}{b_2^2 - b_1^2}\left(\frac{1}{q^2 + b_1^2} - \frac{1}{q^2 + b_2^2}\right) \\ &\quad + \frac{2a_1a_3}{b_3^2 - b_1^2}\left(\frac{1}{q^2 + b_1^2} - \frac{1}{q^2 + b_3^2}\right) \\ &\quad \left. + \frac{2a_2a_3}{b_3^2 - b_2^2}\left(\frac{1}{q^2 + b_2^2} - \frac{1}{q^2 + b_3^2}\right)\right\}\mathrm{d}\Omega_{p_2}, \end{aligned} \tag{7}$$

where $\Omega_{p_2}$ denotes the solid angle of the outgoing electron. The calculation of the integral

$$I_1(b) = \int \frac{\mathrm{d}^3\sigma}{\mathrm{d}k\,\mathrm{d}\Omega_k\,\mathrm{d}\Omega_{p_2}}\left(\frac{q^2}{q^2 + b^2}\right)^2 \mathrm{d}\Omega_{p_2} \tag{8}$$

is greatly facilitated by employing the relation

$$\frac{1}{(q^2 + b^2)^2} = -\frac{\partial}{\partial b^2}\left(\frac{1}{q^2 + b^2}\right). \tag{9}$$

The integral

$$I_2(b) = \int \frac{\mathrm{d}^3\sigma}{\mathrm{d}k\,\mathrm{d}\Omega_k\,\mathrm{d}\Omega_{p_2}}\,\frac{q^4}{q^2 + b^2}\,\mathrm{d}\Omega_{p_2} \tag{10}$$

[1] Since Salvat et al. (1987). have used atomic units, their parameters $\alpha_i$ have to be multiplied by the fine-structure constant $\alpha$ to get the parameters $b_i$ of Eq. (2).

was calculated analytically by Fronsdal and Überall (1958) using the complete Bethe–Heitler cross-section resulting in

$$\begin{aligned} I_2(b) = & -\frac{\alpha Z^2 r_0^2}{2\pi k p_1}\left\{\frac{2p_2}{W^2}(4\varepsilon_1^2+b^2)(\varepsilon_1 D_1/k-2+b^2)\right. \\ & +\frac{L_1}{W}\left[k(D_1+2b^2)\right. \\ & +\frac{2k}{D_1}\{b^4+2b^2(\varepsilon_1^2+p_2^2)-8\varepsilon_1\varepsilon_2\} \\ & +\frac{4\varepsilon_1^2+b^2}{kW^2}\{(D_1+2\varepsilon_1\varepsilon_2-2)D_1 \\ & \left.\left.+b^2(D_1-2\varepsilon_2 k)\}\right] \right. \\ & +\frac{k^2 L_2}{D_1|\mathbf{p}_1-\mathbf{k}|}\left[\frac{2}{D_1}\{4\varepsilon_2^2+b^2(1-D_1)\}\right. \\ & +\frac{1}{2(\mathbf{p}_1-\mathbf{k})^2}\{D_1^2+2D_1(\varepsilon_1\varepsilon_2-1) \\ & \left.\left.+b^2(D_1-2\varepsilon_2 k)\}\right]-\frac{4k}{D_1}\,b^2\,\ln(\varepsilon_2+p_2). \end{aligned} \tag{11}$$

Here $r_0$ denotes the classical electron radius and

$$D_1 = 2(\varepsilon_1 k-\mathbf{k}\cdot\mathbf{p}_1), \tag{12}$$

$$\begin{aligned} W &= [(p_1 D_1/k)^2+2b^2(\varepsilon_1 D_1/k-2)+b^4]^{1/2} \\ &= [(\varepsilon_1 D_1/k-2+b^2)^2+4(\mathbf{p}_1\times\mathbf{k})^2/k^2]^{1/2}, \end{aligned} \tag{13}$$

$$L_1 = \ln\frac{(\varepsilon_1\varepsilon_2-1)D_1/k+\varepsilon_2 b^2+p_2 W}{(\varepsilon_1\varepsilon_2-1)D_1/k+\varepsilon_2 b^2-p_2 W}, \tag{14}$$

$$L_2 = \ln\frac{(|\mathbf{p}_1-\mathbf{k}|+p_2)^2+b^2}{(|\mathbf{p}_1-\mathbf{k}|-p_2)^2+b^2}. \tag{15}$$

By differentiating $I_2(b)$ with respect to $b^2$ one gets after some algebraic manipulations integral (8):

$$\begin{aligned} I_1(b) = & -\frac{\partial I_2}{\partial b^2} \\ = & \frac{\alpha Z^2 r_0^2}{2\pi k p_1}\left\{16p_2(4\varepsilon_1^2+b^2)\frac{(\mathbf{p}_1\times\mathbf{k})^2}{k^2W^4}\right. \\ & -\frac{2p_2}{W^2}[4\varepsilon_1^2+2\varepsilon_1\varepsilon_2-\varepsilon_2 D_1/k \\ & +b^2(1-2\varepsilon_2 k/D_1)] \\ & +\frac{2p_2}{W^2}\,\frac{D_1^2+2(\varepsilon_1\varepsilon_2-1)D_1+b^2(D_1-2\varepsilon_2 k)}{(D_1+b^2)^2+4p_2^2 b^2} \\ & \times\left[\frac{1}{D_1}(16\varepsilon_1\varepsilon_2-4\varepsilon_1^2 b^2-b^4)-\frac{4\varepsilon_1^2+b^2}{k^2W^2}\right. \\ & \left.\times\{D_1^2+2(\varepsilon_1\varepsilon_2-1)D_1+b^2(D_1-2\varepsilon_2 k)\}\right] \\ & -\frac{2k^2 p_2}{(D_1+b^2)^2+4p_2^2 b^2}\left[\frac{4}{D_1^2}\{4\varepsilon_2^2+(1-D_1)b^2\}\right. \\ & +\frac{1}{D_1(\mathbf{p}_1-\mathbf{k})^2}\{D_1^2+2(\varepsilon_1\varepsilon_2-1)D_1 \\ & \left.+b^2(D_1-2\varepsilon_2 k)\}\right]-\frac{4k}{D_1}\ln(\varepsilon_2+p_2) \\ & +\frac{L_1}{W}\left[2k+\frac{4k}{D_1}(\varepsilon_1^2+p_2^2+b^2)\right. \\ & +\frac{2}{D_1 W^2}(\varepsilon_1 D_1-2k+b^2 k)\{8\varepsilon_1\varepsilon_2-D_1^2/2 \\ & -b^2(2\varepsilon_1^2+2p_2^2+D_1)-b^4\} \\ & +\frac{1}{kW^2}\{2(2\varepsilon_1^2+b^2)(D_1-2\varepsilon_2 k)+D_1^2 \\ & +2(\varepsilon_1\varepsilon_2-1)D_1\} \\ & -\frac{3}{kW^4}(4\varepsilon_1^2+b^2)(\varepsilon_1 D_1/k-2+b^2) \\ & \left.\times\{D_1^2+2(\varepsilon_1\varepsilon_2-1)D_1+b^2(D_1-2\varepsilon_2 k)\}\right] \\ & \left.+\frac{k^2 L_2}{D_1|\mathbf{p}_1-\mathbf{k}|}\left[\frac{2}{D_1}-2+\frac{D_1-2\varepsilon_2 k}{2(\mathbf{p}_1-\mathbf{k})^2}\right]\right\}. \end{aligned} \tag{16}$$

Setting $b=0$, i.e., neglecting screening, formula (16) reduces to Sauter's (1934) differential bremsstrahlung cross-section in Born approximation. By means of the integrals $I_1(b)$ and $I_2(b)$, Eq. (7) yields the bremsstrahlung cross-section including screening:

$$\begin{aligned} \frac{\mathrm{d}^2\sigma}{\mathrm{d}k\,\mathrm{d}\Omega_k} = & \sum_{i=1}^{3} a_i^2 I_1(b_i)+\frac{2a_1a_2}{b_2^2-b_1^2}[I_2(b_1)-I_2(b_2)] \\ & +\frac{2a_1a_3}{b_3^2-b_1^2}[I_2(b_1)-I_2(b_3)] \\ & +\frac{2a_2a_3}{b_3^2-b_2^2}[I_2(b_2)-I_2(b_3)]. \end{aligned} \tag{17}$$

The correctness of Eq. (17) was checked by comparison with the results according to Borie (1972). Borie has calculated the cross-section $\mathrm{d}^3\sigma/(\mathrm{d}k\,\mathrm{d}\Omega_k\,\mathrm{d}q)$ in Born approximation. After multiplying this cross-section by $[1-F(q)]^2$ it has to be numerically integrated over the recoil momentum $q$. The results of this procedure are identical to those of Eq. (17). Generally, the atomic screening is most prominent at low photon energies and insignificant near the short-wavelength limit.

Fig. 1 shows the photon angular distribution near forward direction for 10-MeV electrons incident on a gold target and photon energy 3 MeV. For comparison the cross-section in Born approximation without screening is plotted. The screening correction is most pronounced at $\theta=0^\circ$. At larger photon angles, where the cross-section falls off rapidly, the two curves converge. The calculation was performed with the screening parameters of Salvat et al. (1987); those of Moliére (1947) yield similar results.

The photon spectrum $\mathrm{d}\sigma/\mathrm{d}k$ is obtained from Eq. (17) by a single numerical integration over the photon angles. At high energies it is common to use the Bethe (1933) approximation. However, this approximation requires that the energies of both the incident and the final electrons are large, $\varepsilon_1>\varepsilon_2\gg 1$. This condition is not satisfied at the

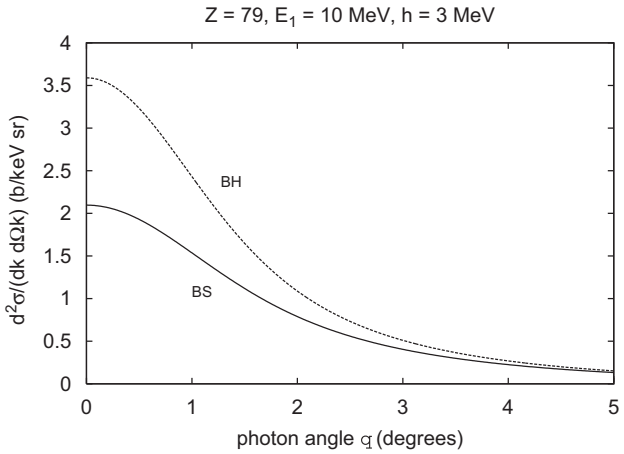


Fig. 1. Photon angular distribution near forward direction for a gold target, incident electron energy $E_1 = 10\,\mathrm{MeV}$, and photon energy $h\nu = mc^2k = 3\,\mathrm{MeV}$. The curve labeled BS is calculated by means of Eq. (17) with the screening parameters of Salvat et al., the dashed curve (BH) depicts the Bethe–Heitler cross-section without screening.

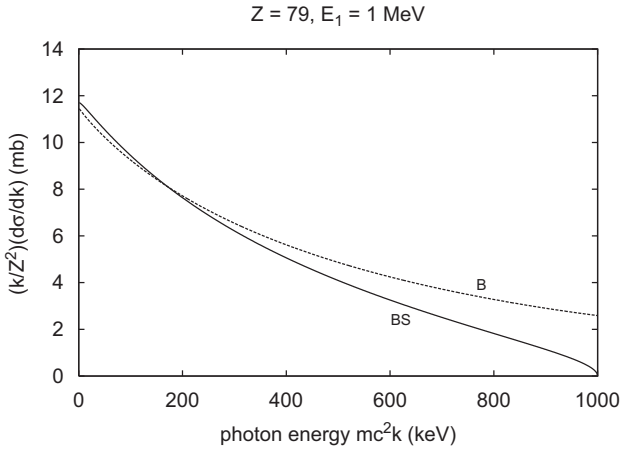


Fig. 2. Scaled photon spectrum for a gold target and incident electron energy $E_1 = 1\,\mathrm{MeV}$. The curve labeled BS is calculated by means of Eq. (17), the dashed curve (B) represents the Bethe approximation.

high-energy part of the spectrum. If only the screening *correction* is calculated, the failure of the Bethe approximation in the vicinity of $\varepsilon_2 = 1$ is not serious at very high energies $\varepsilon_1$ since screening is not important near the tip of the spectrum. Though, for lower energies of the incident electron, the range of validity of the Bethe approximation decreases. Fig. 2 shows the scaled photon spectra from a gold target for incident electrons of $E_1 = 1\,\mathrm{MeV}$ as calculated by numerical integration of Eq. (17) and by the Bethe theory. The screening parameters are from Salvat et al. (1987). The curves agree relatively well up to photon energies of $h\nu \approx 250\,\mathrm{keV}$. At higher values of $h\nu$ where screening is still important, the Bethe cross-section is too high. Of course, the cross-section in Born approximation vanishes at the high-energy limit of the spectrum. This does not matter since the screening correction is negligible near $p_2 = 0$.

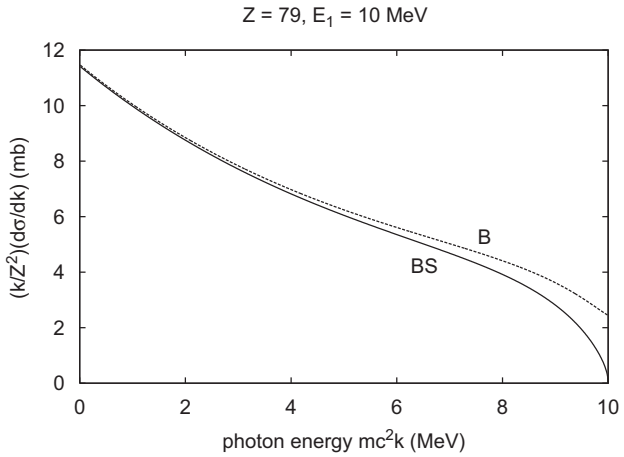


Fig. 3. Same as Fig. 2 for the incident electron energy $E_1 = 10\,\mathrm{MeV}$.

In Fig. 3 are plotted the scaled bremsstrahlung spectra for $E_1 = 10\,\mathrm{MeV}$. At this higher incident electron energy the Bethe approximation yields better results except for the high-energy part of the spectrum.

## 3. Cross-section according to RPD

In order to derive the cross-section of bremsstrahlung beyond the Born approximation we start from the calculation using SM wave functions (Elwert and Haug, 1969). This cross-section is valid for low atomic numbers of the target atoms. At high energies of the incident electrons it is feasible to include high-order Coulomb corrections to the cross-section. Roche et al. (1972) have supplemented the SM wave function by a correction term $\psi_c$:

$$\psi(\mathbf{r}) = \psi_{\mathrm{SM}}(\mathbf{r}) + \psi_c(\mathbf{r}). \tag{18}$$

Designating the two parts of the SM function as

$$\psi_{\mathrm{SM}} = \psi_a + \psi_b, \tag{19}$$

the bremsstrahlung matrix element is composed of

$$M = M_{\mathrm{SM}} + M_{2a,1c} + M_{2b,1b} + M_{2b,1c} + M_{2c,1a} + M_{2c,1b} + M_{2c,1c}, \tag{20}$$

where

$$M_{\mathrm{SM}} = M_{2a,1a} + M_{2a,1b} + M_{2b,1a} \tag{21}$$

and the indices 1 and 2 refer to the incident and outgoing electrons, respectively.

Bethe and Maximon (1954) have shown that at high energies $\varepsilon$ the term $M_{2b,1b}$ gives a contribution of order $\varepsilon^{-2}\ln\varepsilon$ while the contributions of $M_{2a,1c}$ and $M_{2c,1a}$ are of order $1/\varepsilon$, and all the other terms lead to corrections of higher order. Therefore Roche et al. (1972) have restricted themselves to an evaluation of the correction matrix element

$$M_c = M_{2a,1c} + M_{2c,1a}. \tag{22}$$

In this approximation the total matrix element is

$$M = M_{\mathrm{SM}} + M_c \tag{23}$$

leading to

$$|M|^2 = |M_{\mathrm{SM}}|^2 + 2\,\mathrm{Re}(M^*_{\mathrm{SM}} M_c) + |M_c|^2. \tag{24}$$

The resulting cross-section formula can be written as

$$\frac{\mathrm{d}^3\sigma}{\mathrm{d}k\,\mathrm{d}\Omega_k\,\mathrm{d}\Omega_{p_2}} = \frac{\mathrm{d}^3\sigma_1}{\mathrm{d}k\,\mathrm{d}\Omega_k\,d\Omega_{p_2}} + \frac{\mathrm{d}^3\sigma_2}{\mathrm{d}k\,\mathrm{d}\Omega_k\,\mathrm{d}\Omega_{p_2}}. \tag{25}$$

The main term, $\mathrm{d}^3\sigma_1/(\mathrm{d}k\,\mathrm{d}\Omega_k\,\mathrm{d}\Omega_{p_2})$, is identical to the cross-section of Elwert and Haug (1969). The correction term, $\mathrm{d}^3\sigma_2/(\mathrm{d}k\,\mathrm{d}\Omega_k\,\mathrm{d}\Omega_{p_2})$, is obtained from the second and the third term of the matrix element squared (24). The cross-sections have the form (Roche et al., 1972)

$$\begin{aligned}
&\frac{\mathrm{d}^3\sigma_1}{\mathrm{d}k\,\mathrm{d}\Omega_k\,\mathrm{d}\Omega_{p_2}} \\
&= \frac{\alpha Z^2 r_0^2}{\pi^2}\frac{kp_2}{p_1} N\{[\varepsilon_1\varepsilon_2 - 1 \\
&\quad - (\hat{\mathbf{k}}\cdot\mathbf{p}_1)(\hat{\mathbf{k}}\cdot\mathbf{p}_2)]|J_1|^2 \\
&\quad + [\varepsilon_1\varepsilon_2 + 1 + (\hat{\mathbf{k}}\cdot\mathbf{p}_1)(\hat{\mathbf{k}}\cdot\mathbf{p}_2)](|\mathbf{J}_2|^2 + |\mathbf{J}_3|^2) \\
&\quad + 2\,\mathrm{Re}[(\mathbf{J}_3^* - \mathbf{J}_2^*)\cdot\{\mathbf{p}_1(\mathbf{J}_2\cdot\hat{\mathbf{k}})(\mathbf{p}_2\cdot\hat{\mathbf{k}}) \\
&\quad - \mathbf{p}_2(\mathbf{J}_3\cdot\hat{\mathbf{k}})(\mathbf{p}_1\cdot\hat{\mathbf{k}})\} \\
&\quad - (\varepsilon_1\varepsilon_2 + 1 + \mathbf{p}_1\cdot\mathbf{p}_2)(\mathbf{J}_2\cdot\hat{\mathbf{k}})(\mathbf{J}_3^*\cdot\hat{\mathbf{k}}) \\
&\quad + (\mathbf{J}_2\cdot\mathbf{p}_1)(\mathbf{J}_3^*\cdot\mathbf{p}_2) - (\mathbf{J}_2\cdot\mathbf{p}_2)(\mathbf{J}_3^*\cdot\mathbf{p}_1) \\
&\quad + \varepsilon_1 J_1^*\{\mathbf{J}_3\cdot\mathbf{p}_2 - (\mathbf{J}_2\cdot\hat{\mathbf{k}})(\mathbf{p}_2\cdot\hat{\mathbf{k}})\} \\
&\quad + \varepsilon_2 J_1^*\{\mathbf{J}_2\cdot\mathbf{p}_1 - (\mathbf{J}_3\cdot\hat{\mathbf{k}})(\mathbf{p}_1\cdot\hat{\mathbf{k}})\} \\
&\quad + (\mathbf{J}_2\cdot\mathbf{J}_3^*)\{\mathbf{p}_1\cdot\mathbf{p}_2 - (\hat{\mathbf{k}}\cdot\mathbf{p}_1)(\hat{\mathbf{k}}\cdot\mathbf{p}_2)\}]\},
\end{aligned} \tag{26}$$

$$\begin{aligned}
&\frac{\mathrm{d}^3\sigma_2}{\mathrm{d}k\,\mathrm{d}\Omega_k\,\mathrm{d}\Omega_{p_2}} \\
&= \alpha^2 Z^3 r_0^2 \frac{kp_2(\mathbf{q}\cdot\mathbf{k})}{p_1 q D_1 D_2} N \\
&\quad \times \left\{\frac{2}{\pi}\,\mathrm{Re}[(\{\varepsilon_1\varepsilon_2 - 1 - (\hat{\mathbf{k}}\cdot\mathbf{p}_1)(\hat{\mathbf{k}}\cdot\mathbf{p}_2)\}J_1\right. \\
&\quad + \varepsilon_1\{\mathbf{J}_3\cdot\mathbf{p}_2 - (\mathbf{J}_2\cdot\hat{\mathbf{k}})(\mathbf{p}_2\cdot\hat{\mathbf{k}})\} \\
&\quad + \varepsilon_2\{\mathbf{J}_2\cdot\mathbf{p}_1 - (\mathbf{J}_3\cdot\hat{\mathbf{k}})(\mathbf{p}_1\cdot\hat{\mathbf{k}})\})\mathrm{e}^{\mathrm{i}\Phi}] \\
&\quad \left. + \alpha Z\frac{\mathbf{q}\cdot\mathbf{k}}{qD_1D_2}[\varepsilon_1\varepsilon_2 - 1 - (\hat{\mathbf{k}}\cdot\mathbf{p}_1)(\hat{\mathbf{k}}\cdot\mathbf{p}_2)]\right\},
\end{aligned} \tag{27}$$

where $\hat{\mathbf{k}} = \mathbf{k}/k$ denotes a unit vector and

$$N = \frac{4\pi^2 a_1 a_2}{(\mathrm{e}^{2\pi a_1} - 1)(1 - \mathrm{e}^{-2\pi a_2})}, \tag{28}$$

$$a_1 = (\varepsilon_1/p_1)\alpha Z, \quad a_2 = (\varepsilon_2/p_2)\alpha Z, \tag{29}$$

$$\begin{aligned}
J_1 &= 2\left(\frac{\varepsilon_2}{D_1} - \frac{\varepsilon_1}{D_2}\right)\frac{V + \mathrm{i}a_2 x W}{q^2} \\
&\quad + 2\mathrm{i}\frac{(1-x)W}{D_1 D_2}[\varepsilon_1 a_2(\mu/D_2 - 1) \\
&\quad - \varepsilon_2 a_1(\mu/D_1 + 1)],
\end{aligned} \tag{30}$$

$$\begin{aligned}
\mathbf{J}_2 &= \frac{V + \mathrm{i}a_2 x W}{D_2 q^2}\mathbf{q} \\
&\quad - \frac{\mathrm{i}a_2(1-x)W}{D_1 D_2}[(\mu/D_2 - 1)\,\mathbf{q} - \mathbf{P}/p_1],
\end{aligned} \tag{31}$$

$$\begin{aligned}
\mathbf{J}_3 &= \frac{V + \mathrm{i}a_2 x W}{D_1 q^2}\mathbf{q} \\
&\quad - \frac{\mathrm{i}a_1(1-x)W}{D_1 D_2}[(\mu/D_1 + 1)\,\mathbf{q} - \mathbf{P}/p_2],
\end{aligned} \tag{32}$$

$$V = F(-\mathrm{i}a_1,\ \mathrm{i}a_2; 1; x), \tag{33}$$

$$W = F(1 - \mathrm{i}a_1,\ 1 + \mathrm{i}a_2; 2; x), \tag{34}$$

$$x = 1 - \frac{D_1 D_2}{\mu q^2}, \tag{35}$$

$$D_1 = 2(\varepsilon_1 k - \mathbf{k}\cdot\mathbf{p}_1), \quad D_2 = 2(\varepsilon_2 k - \mathbf{k}\cdot\mathbf{p}_2), \tag{36}$$

$$\mu = 2(\varepsilon_1\varepsilon_2 + p_1 p_2 - 1), \quad \mathbf{P} = p_1\mathbf{p}_2 + p_2\mathbf{p}_1, \tag{37}$$

$$\Phi = a_1\ \ln(q^2/D_2) - a_2\ \ln(\mu/D_2). \tag{38}$$

The hypergeometric functions $V$ and $W$ differ from those of Elwert and Haug (1969) in that their argument $x$ is $0 \leqslant x < 1$ which is advantageous in numerical evaluations. For that reason the functions $J_1$, $\mathbf{J}_2$, and $\mathbf{J}_3$ are different from the functions $I_1/K_1$, $\mathbf{I}_2/K_1$, and $\mathbf{I}_3/K_1$ of Elwert and Haug (1969).

Comparison of photon spectra computed by numerical integration of (25) shows good agreement with experimental data even for targets with high atomic numbers. Deviations at the low-energy part of the spectra are probably due to the neglect of atomic screening in the calculation. Roche et al. (1972) have found that the part of order $\alpha^2 Z^3$ of the correction term (27) yields values smaller than those given by the part of order $\alpha^3 Z^4$. Moreover, the cross-section displays a correct behavior near the high-frequency limit of the spectrum where the Born-approximation formula fails (see below).

Fig. 4 shows the photon angular distribution near forward direction for a gold target ($Z = 79$), incident electrons of 10 MeV, and photon energy 7 MeV. For comparison the cross-section in Born approximation is displayed. The Coulomb correction is most distinct near the forward angle $\theta = 0^\circ$. At larger angles, where the two curves converge, the cross-section decreases rapidly due to relativistic beaming.

The screening correction to the cross-section of Roche et al. (1972) is performed by applying the result of Olsen et al. (1957) that the bremsstrahlung cross-section integrated over the motion of the final electron is additive at high

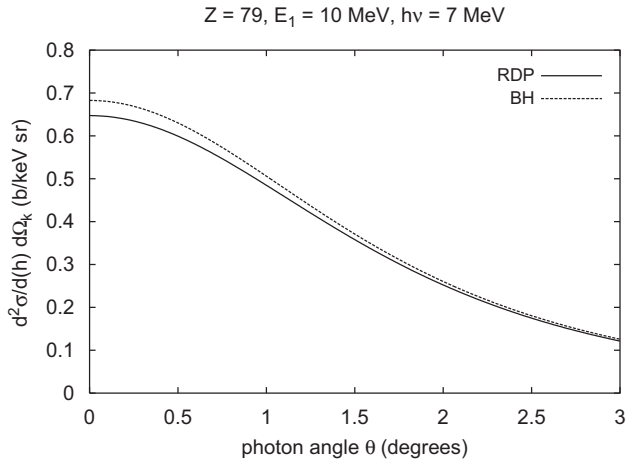


Fig. 4. Photon angular distribution for a gold target, incident electron energy $E_1 = 10\,\mathrm{MeV}$, and photon energy $h\nu = 7\,\mathrm{MeV}$. The cross-section of Roche et al. (RDP) is compared with that of Bethe and Heitler (BH).

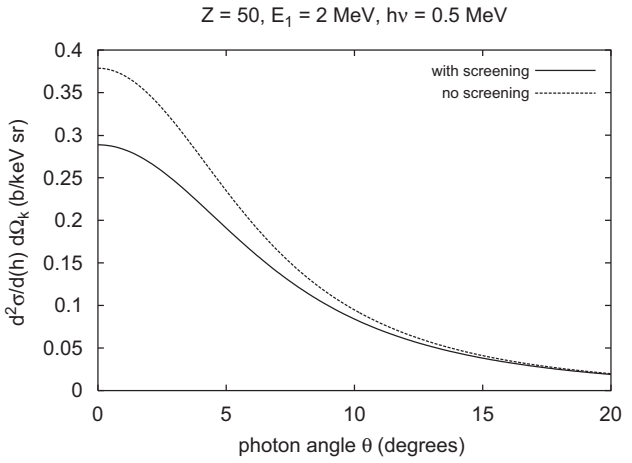


Fig. 5. Photon angular distribution for a tin target, incident electron energy $E_1 = 2\,\mathrm{MeV}$, and photon energy $h\nu = 0.5\,\mathrm{MeV}$. The cross-section of Roche et al. (1972) is shown with and without screening correction.

energies, i.e., Coulomb and screening corrections are independent of each other:

$$\left(\frac{\mathrm{d}^2\sigma}{\mathrm{d}k\,\mathrm{d}\Omega_k}\right)^{\text{screened}}_{\text{exact}} \approx \left(\frac{\mathrm{d}^2\sigma}{\mathrm{d}k\,\mathrm{d}\Omega_k}\right)^{\text{no screening}}_{\text{exact}} + \left[\left(\frac{\mathrm{d}^2\sigma}{\mathrm{d}k\,\mathrm{d}\Omega_k}\right)^{\text{screened}}_{\text{Born}} - \left(\frac{\mathrm{d}^2\sigma}{\mathrm{d}k\,\mathrm{d}\Omega_k}\right)^{\text{no screening}}_{\text{Born}}\right]. \quad (39)$$

Thus, one simply adds the effect of screening as calculated in Born approximation (see Section 2) to the RDP cross-section (25). The second term put in brackets on the right-hand side of (39) is the (negative) difference between Eq. (17) and Sauter's (1934) doubly differential cross-section. The same procedure holds for the photon spectrum $\mathrm{d}\sigma/\mathrm{d}k$.

The choice of the RDP cross-section (25) as the "exact" unscreened cross-section in Eq. (39) is justified for the following reasons:

(1) For low atomic numbers $Z$ the first term of Eq. (25) has been shown by Fink and Pratt (1973) to be a significant improvement over the Born approximation. In particular, the cross-section remains finite at the short-wavelength limit $p_2 = 0$.
(2) At high energies the first term of Eq. (25) is a good approximation even for high atomic numbers (Bethe and Maximon, 1954). Moreover, the additional assumptions of Bethe and Maximon are not made, viz., to drop terms of relative order $1/\varepsilon^2$ and $1/k^2$, and to use the small-angle approximation. The second term of Eq. (25) provides a supplementary correction for high values of $Z$ and was shown by Roche et al. (1972) to improve the agreement with experimental data.

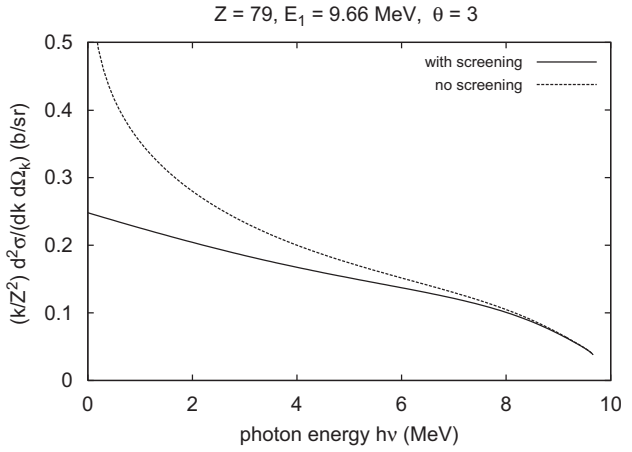


Fig. 6. Scaled cross-section for a gold target, incident electrons of 9.66 MeV, and photon angle $\theta = 3^\circ$. The cross-section of Roche et al. (1972) is shown with and without screening correction.

In Fig. 5 is displayed the photon angular distribution near forward direction as calculated by means of Eq. (39) for a tin target ($Z = 50$), incident electrons of 2 MeV, and photon energy $h\nu = 0.5\,\mathrm{MeV}$. In comparison with the dashed curve showing the RDP cross-section, Eq. (25), the large effect of screening near the photon angle $\theta = 0^\circ$ is conspicuous.

The effect of screening on the spectrum of photons emitted into a certain direction is depicted in Fig. 6 for the parameters of an experiment performed by Starfelt and Koch (1956). The dashed curve is calculated by means of the RDP cross-section differential with respect to photon energy and angle. It is seen that the unscreened cross-section can be only applied near the high-energy part of the spectrum.

The bremsstrahlung cross-section for high incident electron energies, differential in the photon energy and

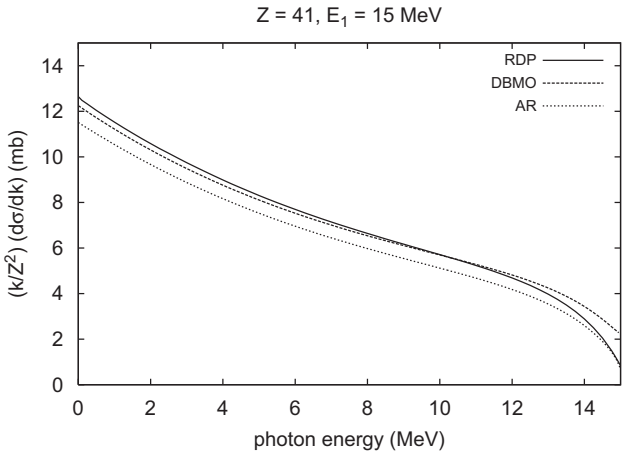


Fig. 7. Scaled bremsstrahlung cross-section including screening correction for $Z = 41$ (Nb) and incident electron energy $E_1 = 15$ MeV. RDP: present theory; DBMO: Davies et al., Olsen; AR: Al-Beteri and Raeside.

including form-factor screening and Coulomb corrections, has been calculated by a number of authors. An often used approach is the DBMO formula resulting from the work of Davies et al. (1954) and Olsen (1955) (see Tseng and Pratt, 1979). It is believed that this calculation is valid for $E_1 > 15-50$ MeV (depending on $Z$) and $\varepsilon_2 \gg 1$. A similar formula was derived by Sørenssen (1965). Seltzer and Berger (SB, 1985) tabulated a comprehensive set of data obtained through the synthesis of various theoretical results. They are considered to constitute the best available bremsstrahlung spectra yet, including the contribution of electron–electron bremsstrahlung. The present cross-sections are in excellent agreement with those of SB for targets with low and intermediate atomic numbers, except for the neighborhood of the high-energy limit. Al-Beteri and Raeside (AR, 1989) have derived an empirical formula for the cross-section in the MeV range exhibiting better agreement with experiment than existing bremsstrahlung cross-sections over wide ranges of electron energies and target atomic numbers. The partial-wave formalism can only be applied up to incident electron energies of $E_1 \approx 2$ MeV. In order to bridge the gap between the results for $E_1 \leqslant 2$ MeV and the DBMO approach, Tseng and Pratt (1979) used a partial-wave interpolation method to calculate the bremsstrahlung energy spectra from atoms with $Z = 13$ and 92 for $E_1 = 5$ and 10 MeV. The cross-sections of the present calculations compare favorably with those of Tseng and Pratt for the low atomic number $Z = 13$ down to $E_1 = 1$ MeV. For $Z = 92$ there are larger discrepancies, especially near the high-energy limit of the spectrum.

A comparison of some of these cross-sections is displayed in Fig. 7 for $Z = 41$ (Nb) and incident electrons of 15 MeV.[2] The data of SB would not be distinguishable from the present ones (RDP) except for the neighborhood of the high-energy limit. It is interesting to note that the AR values are systematically lower than the RDP, DBMO, and SB cross-sections.

[2]The cross-sections of Fig. 7 do not include the contribution of bremsstrahlung in the field of atomic electrons.

Table 1
Bremsstrahlung cross-sections $d\sigma/d(h\nu)$ in units of b/MeV including screening correction for $Z = 74$ (W) and electron energy $E_1 = 50$ MeV

| $h\nu$ (MeV) | 10 | 15 | 20 | 25 | 30 | 35 | 40 | 45 | 50 |
|---|---|---|---|---|---|---|---|---|---|
| RDP | 5.04 | 3.06 | 2.11 | 1.566 | 1.225 | 0.990 | 0.805 | 0.609 | 0.162 |
| SB | 4.84 | 2.94 | 2.03 | 1.508 | 1.183 | 0.961 | 0.789 | 0.614 | 0.137 |
| DBMO | 4.80 | 2.91 | 2.01 | 1.499 | 1.176 | 0.955 | 0.782 | 0.601 | 0.199 |
| AR | 4.89 | 2.97 | 2.05 | 1.523 | 1.191 | 0.961 | 0.780 | 0.588 | 0.132 |

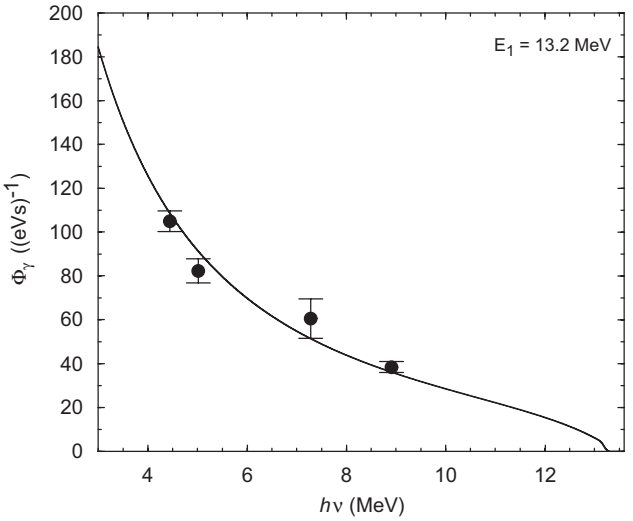


Fig. 8. Spectral photon flux determined in an experiment investigating photon-induced reactions. The bremsstrahlung photons were produced by 13.2-MeV electrons impinging on a niobium target ($Z = 41$). The curve calculated by means of the RDP cross-section with screening correction was fitted to the experimental points.

For very high energies of the incident electrons the SB cross-sections are close to the values of DBMO up to 90% of the high-energy limit, whereas the present data (RDP) are a little higher. Table 1 shows a sample of cross-sections for 50-MeV electron impinging on a tungsten target ($Z = 74$).

Most of the measurements of bremsstrahlung cross-sections were performed many decades ago (see Al-Beteri and Raeside, 1989) and are subject to large experimental errors. The present calculations were applied to recent experiments using photon-induced reactions (Schwengner et al., 2005). The bremsstrahlung was produced by 13.2-MeV electrons impinging on a thin niobium target ($Z = 41$). The proton spectra originating from the photo-disintegration of deuterons were used to derive the photon spectra. In another experiment (Schwengner et al., 2007) the photon-scattering target was combined with $^{11}$B atoms in order to determine the absolute photon flux. Fig. 8 shows the spectral photon flux $\Phi_\gamma$ calculated by means of the RDP cross-section with screening correction.

The theoretical flux curve was fitted to the four experimental points representing the absolute flux at excitation energies of the $^{11}$B nucleus.

At the short-wavelength limit ($p_2 = 0$) the argument $x$ of the hypergeometric functions $V$ and $W$ tends to zero and $a_2 \to \infty$. The product $a_2 x$ takes the finite value

$$a\xi = \lim_{p_2 \to 0} a_2 x = 2a \frac{p_1}{D_1} \{\varepsilon_1 - \mathbf{k} \cdot \mathbf{p}_1 - \hat{\mathbf{p}}_1 \cdot \hat{\mathbf{p}}_2 + (p_1 - \mathbf{k} \cdot \hat{\mathbf{p}}_1)\, \mathbf{k} \cdot \hat{\mathbf{p}}_2\}. \quad (40)$$

Therefore, the functions $V$ and $W$ transform to the confluent hypergeometric functions $V_0$ and $W_0$:

$$V \to V_0 = F(-\mathrm{i}a_1; 1; \mathrm{i}a\xi), \quad (41)$$

$$W \to W_0 = F(1 - \mathrm{i}a_1; 2; \mathrm{i}a\xi). \quad (42)$$

For $p_2 = 0$ cross-section (26) is still a good approximation at low atomic numbers $Z$ (Fink and Pratt, 1973). However, the correction term (27) is no longer reliable since the assumption $\varepsilon_2 \gg 1$ does not hold there. For the high-frequency end of the bremsstrahlung spectrum there exist two analytical calculations for the limit $\varepsilon_1 \to \infty$ including higher-order Coulomb corrections. Using an exact wave function for the final electron state, Deck et al. (1964) have evaluated the cross-section to the first three nonvanishing orders in $\alpha Z$. Jabbur and Pratt (1963, 1964) started from the relationship between the atomic photoeffect and the tip region of the bremsstrahlung spectrum. They gave expressions for the cross-sections $\sigma_{jl}$ for $s$, $p$, and $d$ final angular momentum states, including a double integral which was expanded into a power series in $a = \alpha Z$ up to relative order $a^3$. The two methods yield results which are nearly equal for low-$Z$ elements, differ by 3% for Ag ($Z = 47$), and about 12% for $U(Z = 92)$. It is to be expected that the cross-sections of Jabbur and Pratt are most accurate. Their numerical results are easily reproduced by multiplying their analytical results by a correction factor given by Seltzer and Berger (1985). The latter authors also suggested an interpolation method to get results for lower values of the incident electron energy.

## Acknowledgment

The author is indebted to Dr. R. Schwengner for providing Fig. 8.

## References

Al-Beteri, A.A., Raeside, D.E., 1989. An improved electron bremsstrahlung cross-section formula for Monte-Carlo transport simulation. Nucl. Instrum. Methods Phys. Res. B 44, 149–157.

Bethe, H.A., 1933. The influence of screening on the creation and stopping of electrons. Proc. Cambridge Philos. Soc. 30, 524.

Bethe, H.A., Heitler, W., 1934. On the stopping of fast particles and on the creation of positive electrons. Proc. R. Soc. London A 146, 83.

Bethe, H.A., Maximon, L.C., 1954. Theory of bremsstrahlung and pair production. I. Differential cross section. Phys. Rev. 93, 768–784.

Borie, E., 1972. Screening and second Born corrections to bremsstrahlung at intermediate energies. Nuovo Cimento 11A, 969–982.

Davies, H., Bethe, H.A., Maximon, L.C., 1954. Theory of bremsstrahlung and pair production. II. Integral cross section for pair production. Phys. Rev. 93, 788–795.

Deck, R.T., Mullin, C.J., Hammer, C.L., 1964. High-frequency limit of the bremsstrahlung spectrum. Nuovo Cimento 32, 180–197.

Elwert, G., Haug, E., 1969. Calculation of bremsstrahlung cross sections with Sommerfeld—Maue eigenfunctions. Phys. Rev. 183, 90–105.

Fink, J.K., Pratt, R.H., 1973. The use of Furry–Sommerfeld–Maue wave functions in pair production and bremsstrahlung. Phys. Rev. A 7, 392–403.

Fronsdal, C., Überall, H., 1958. Polarization of bremsstrahlung from polarized electrons. Phys. Rev. 111, 580–586.

Haug, E., Nakel, W., 2004. The Elementary Process of Bremsstrahlung. World Scientific, Singapore.

Heitler, W., 1954. The Quantum Theory of Radiation, third ed. Oxford University Press, Oxford.

Jabbur, R.J., Pratt, R.H., 1963. High-frequency region of the spectrum of electron and positron bremsstrahlung. Phys. Rev. 129, 184–190.

Jabbur, R.J., Pratt, R.H., 1964. High-frequency region of the spectrum of electron and positron bremsstrahlung. II. Phys. Rev. 133B, 1090–1091.

Moliére, G., 1947. Theorie der Streuung schneller geladener Teilchen. Einzelstreuung am abgeschirmten Coulomb-Feld. Z. Naturforsch. 2a, 133–145.

Olsen, H., 1955. Outgoing and ingoing waves in final states and bremsstrahlung. Phys. Rev. 99, 1335–1336.

Olsen, H., Maximon, L.C., Wergeland, H., 1957. Theory of high-energy bremsstrahlung and pair production in a screened field. Phys. Rev. 106, 27–46.

Roche, G., Ducos, C., Proriol, J., 1972. Bremsstrahlung cross-section formula including a high-order Coulomb correction. Phys. Rev. A 5, 2403–2408.

Salvat, F., Martínez, J.D., Mayol, R., Parellada, J., 1987. Analytical Dirac–Hartree–Fock–Slater screening function for atoms ($Z = 1-92$). Phys. Rev. A 36, 467–474.

Sauter, F., 1934. Über die Bremsstrahlung schneller Elektronen. Ann. Phys. (Leipzig) 20, 404–412.

Schwengner, R., Beyer, R., Dönau, F., et al., 2005. The photon-scattering facility at the superconducting electron accelerator ELBE. Nucl. Instrum. Methods Phys. Res. A 555, 211–219.

Schwengner, R., Rusev, G., Benouaret, N., et al., 2007. Dipole response of $^{88}$Sr up to the neutron-separation energy. Phys. Rev. C 76, 034321.

Seltzer, S.M., Berger, M.J., 1985. Bremsstrahlung spectra from electron interactions with screened atomic nuclei and orbital electrons. Nucl. Instrum. Methods Phys. Res. B 12, 95–134.

Sørenssen, A., 1965. The influence of electronic screening on high-energy bremsstrahlung and pair production. Nuovo Cimento 38, 745–770.

Starfelt, N., Koch, H.W., 1956. Differential cross-section measurements of thin-target bremsstrahlung produced by 2.7- to 9.7-MeV electrons. Phys. Rev. 102, 1598–1612.

Tseng, H.K., Pratt, R.H., 1971. Exact screened calculations of atomic-field bremsstrahlung. Phys. Rev. A 3, 100–115.

Tseng, H.K., Pratt, R.H., 1979. Electron bremsstrahlung energy spectra above 2 MeV. Phys. Rev. A 19, 1525–1528.